General Disclaimer

One or more of the Following Statements may affect this Document

- This document has been reproduced from the best copy furnished by the organizational source. It is being released in the interest of making available as much information as possible.

- This document may contain data, which exceeds the sheet parameters. It was furnished in this condition by the organizational source and is the best copy available.

- This document may contain tone-on-tone or color graphs, charts and/or pictures, which have been reproduced in black and white.

- This document is paginated as submitted by the original source.

- Portions of this document are not fully legible due to the historical nature of some of the material. However, it is the best reproduction available from the original submission.

NASA Technical Memorandum 79077

MECHANISMS OF BORON FIBER STRENGTHENING BY THERMAL TREATMENT

J. A. DiCarlo
Lewis Research Center
Cleveland, Ohio

TECHNICAL PAPER presented at the
Third Annual Conference in Composites and Advanced Materials
sponsored by the Ceramic-Metal Systems Division of the
American Ceramic Society
Merritt Island, Florida, January 21-24, 1979

MECHANISMS OF BORON FIBER STRENGTHENING BY THERMAL TREATMENT

by J. A. DiCarlo

National Aeronautics and Space Administration
Lewis Research Center
Cleveland, Ohio

ABSTRACT

The fracture strain for boron on tungsten fibers can be improved by heat treatment under vacuum or argon environments. The mechanical basis for this improvement is thermally-induced axial contraction of the entire fiber, whereby strength-controlling core flaws are compressed and fiber fracture strain increased by the value of the contraction strain. By highly sensitive measurements of fiber density and volume, the physical mechanism responsible for contraction under both environments was identified as boron atom diffusion out of the fiber sheath. The fiber contracts because the average volume of the resulting microvoid was determined to be only 0.26±0.09 the average atomic volume of the removed atom. The basic and practical implications of these results are discussed with particular emphasis on the theory, use, and limitations of heat-induced contraction as a simple cost-effective secondary processing method.

E-9894

INTRODUCTION

In a previous report it was demonstrated that the fracture parameters for commercial boron on tungsten fibers could be significantly improved by simple secondary processing methods (1). These methods were based on the observation that the two major sources for fracture of commercial 203 μm diameter fibers were flaws within the as-fabricated surface layer and flaws within the 17 μm diameter tungsten boride core (2). The surface flaws were found to control the as-received

fracture parameters of 3.6 GN/m^2 for the average fracture strength σ_F and ~20% for the strength coefficient of variability (COV). Once surface flaws were removed by a slight etch, essentially all fractures were observed to be core flaw-initiated and the fracture parameters improved significantly to $\sigma_F = 4.3$ GN/m^2 and COV $< 5\%$. To produce further improvement, secondary processing methods were utilized which took advantage of physical mechanisms operating within the boron sheath to induce axial contraction of the entire fiber and compression of the elastic core. In these cases σ_F was increased by an amount equal to $E\epsilon_z$ where E is the fiber modulus and ϵ_z is the process-induced axial contraction strain. Thus for the easily attained ϵ_z value of 0.3%, the σ_F for processed fibers was observed to increase to 5.5 GN/m^2. Because fracture was still controlled by core flaws, the COV remained at the low core-related value of less than 5%.

Four methods were employed to produce fiber contraction. These were discriptively labelled as Etch, Etch-Heat, Heat-Vacuum, and Heat-Argon. The Etch method consisted of surface layer removal by immersion of the as-received commercial fiber in nitric acid near 100° C. This process not only eliminated flaws in the as-fabricated surface but also produced fiber contraction due to elastic relaxation of residual stresses within the bulk of the boron sheath (3). In the Etch-Heat method the etched fiber was subsequently heat treated to 700° C, producing additional contraction by thermally-induced anelastic relaxation of the residual stresses (1). Total axial contraction available from the two etch methods was about 0.2%.

For the Heat-Vacuum method the as-received fiber was heated under high vacuum between 700° and 1200° C. This treatment not only produced large contractions (over 1%) but also resulted in the growth of surface crystals which had to be eliminated by a deep final etch. To avoid the crystal problem, the Heat-Argon method was developed in which commercial fibers were resistively heated to 1000° C in argon gas. This method not only left the fiber surface visibly unchanged but also produced large axial contractions (over 0.8%) at a faster rate than the Heat-Vacuum method. In contrast to the two Etch methods in which contraction could be attributed to residual stresses, the physical mechanisms controlling

contraction in the Heat-Vacuum and Heat-Argon were undetermined. Nevertheless, for contraction strains up to 0.3%, a one-to-one relationship was found between the ϵ_z value and the increase in fiber fracture strain. However, for ϵ_z greater than 0.3%, deterioriation in fracture strain was observed rather than improvement.

Recognizing the possible potential of secondary heat treatment as a simple strength improvement technique, our primary goal in this study was to identify the physical mechanisms responsible for the axial contractions observed during Heat-Vacuum and Heat-Argon processing. It was anticipated that such identification would explain not only the large contraction strains available from these processing methods but also the apparent practical limit of 0.3% for improving fracture strain. An understanding of contraction was especially important for the Heat-Argon method which appeared to be cost-effective (1). Because a possible contraction mechanism was considered to be thermally-induced fiber densification, the principal experimental tool of this work was a liquid density gradient column which was used for highly accurate measurements of boron fiber density as a function of contraction. Wherever possible, the density and axial strain data were augmented with radial strain data to ascertain volumetric changes and develop plausible models.

EXPERIMENTAL

The specimens used in this study were 203 μm (8 mil) diameter commercial fibers produced by Avco Systems Division. These fibers were chemically vapor deposited in a single stage reactor by the hydrogen reduction of boron trichloride onto a resistively heated tungsten wire substrate which passed continuously through the reactor (4). During deposition the original 13 μm (0.5 mil) tungsten substrate became completely borided to form a 17 μm (0.67 mil) diameter core with two phases: W_2B_5 and a mixture of WB_4 and boron (5).

For the Heat-Vacuum method, a batch of as-received fiber specimens with lengths of ~80 mm were supported vertically in open-ended 20 mm long quartz tubes (1) and then heat-treated for various times between 900°

and 1200° C in a high vacuum furnace (10^{-7} to 10^{-6} torr). Before and after heating, the lengths of two to four different fibers were measured to ±0.003 mm with a traveling optical microscope in order to determine the heat-induced axial contraction strain.

For the Heat-Argon method, long single fibers were held vertically in a static reactor similar to that employed for fiber production (1). With nominally pure argon gas (99.995%) flowing at one atmosphere through the reactor, the fibers were resistance heated for various times between 800° and 1000° C. Fiber axial contractions at temperature were measured continuously with a traveling microscope located at the fiber end protruding from the bottom cap of the reactor. The heated fiber lengths were varied between 16 and 60 cm in order to determine and correct for any effects from non-heated portions on axial strain measurements. Argon flow rates between 20 and 200 cm^3/min were employed with no apparent effects on heat-induced contractions. For both heat treatment methods, temperature was measured with an optical pyrometer.

During the course of the reactor studies, it was observed that for temperatures greater than 1000° C, fiber breakage would occur in about 2 minutes at the top jewel which separated the heated fiber from the mercury reservoir. Because impurities in the argon were considered a possible source of the premature breakage, a hot titanium getter (900° C) was inserted in the argon gas line to reduce the impurity level. This procedure, however, did not eliminate the problem, making it necessary to employ furnace heating in order to process fibers at temperatures over 1000° C in argon. Thus, as in the Heat-Vacuum method, 80 mm long fibers were placed into quartz tubes and then inserted into a furnace containing either "pure" or Ti-gettered argon.

For accurate measurement of the density of the fibers before and after contraction, a liquid density gradient column was prepared according to ASTM test D 1505 (Method C). Final density distribution ranged from 2.25 to 2.50 g/cm^3 with a gradient of 0.0003 g/cm^3 per mm of column height. Linearity was excellent as evidenced by five evenly spaced calibration floats accurate to 0.0001 g/cm^3. Before each measurement the ends of the fiber were mechanically squared as much as possible in

order to avoid density errors caused by overexposure or underexposure of the highly dense core region. However, for the fiber lengths employed (2 to 3 cm), it was estimated that unprepared fiber ends would at worst produce a density error of only 0.0005 g/cm^3 (as measured at the fiber's center of gravity).

To develop a theory for the density and contraction data of the Heat-Argon method, it was necessary to make accurate fiber diameter measurements before and after heat treatment. Because of the rough surface and small diameter of the fibers, optical measurements could not achieve the required accuracy. For this reason effective diameter determinations were made by combining the highly accurate density measurements with highly accurate mass and length measurements. The typical procedure was first to measure length of approximately 30 mm long fiber specimens with the traveling microscope (error = 1×10^{-4}). The specimens were then weighed on a sensitive (0.1 μg) electrobalance (error = 5×10^{-5}). Finally the specimens were inserted into the density column (error = 1×10^{-4}). Thus, the effective diameter measurements were estimated to have an error of less than 2×10^{-4}.

RESULTS AND DISCUSSION

Heat-Vacuum Method

Table 1 lists axial strain and density data for as-received 203 μm diameter boron fibers after heat treatment under high vacuum. Each specimen was cleaned in methanol before heat treatment and before density measurement. Due to the low vapor pressure of boron (6), it was assumed that negligible loss of fiber mass occurred during the vacuum processing. The initial axial strain of the as-received fiber was taken to be zero. Treatment-induced strains were considered negative if contractive and positive if expansive. Density of the as-received fibers was determined to be 2.4099±0.0003 gm/cm^3. This density was due in most part to an average density of 2.3465 g/cm for the amorphous boron

sheath (5). The small core contribution to the density data (+0.0634 gm/cm^3) was assumed to remain constant during processing because no changes were observed in the core diameter as measured optically. The one density data point over 2.50 gm/cm^3 was determined from extrapolation of exponential time-of-fall data through the density column. Also included in Table 1 are density data after vacuum heat-treatment at 1320^o and 1700^o C where recrystallization effects are known to occur in the amorphous boron sheath (7, 8).

From the ϵ_z data of Table 1, it is clear that the Heat-Vacuum contraction was controlled by a thermally-activated mechanism. That is, for constant processing time, small temperature changes produced large increases in contraction. This behavior is also evident in Fig. 1 where the ϵ_z data are plotted versus the various time-temperature conditions. The fact that an order of magnitude change in processing time shifted the ϵ_z curves by the same $1/T$ amount indicates that the mechanisms responsible for contractions between 0.3 and 1.0% were controlled by a single activation energy. In our previous report (1), we employed the data of Fig. 1 to determine that this energy was 3.1±0.2 eV. There was insufficient data for determining activation energies for contractions below 0.3%.

Regarding density changes during Heat-Vacuum processing, the Fig. 2 plot of density ρ versus contraction strain indicates that ρ was dependent only on the magnitude of ϵ_z and was independent of the time-temperature conditions employed to obtain ϵ_z. For contractions less than 0.4%, no increase in density was observed. To the contrary, the data near 0.2% suggest a slight drop in density. Thus, during the early stages of vacuum processing, fiber contraction was not accompanied by an increase in fiber density but perhaps by a slight decrease. A possible mechanistic model to account for these observations could be as follows.

During initial processing when contraction strains were low, boron atoms diffused out of the sheath onto the fiber surface, leaving microvoids within the amorphous sheath. The atoms surrounding the microvoids relaxed to partially fill the microvoid volume, thereby producing axial and radial contraction and a smaller fiber density. The radial contraction would not be observable because the extra boron atoms on the

surface produced a net increase in fiber diameter. The extra atoms on the fiber end surfaces had negligible effect on the axial contraction measurements because the estimated added thickness is of the order of 1 μm and the measured length change was of the order of 10^3 μm.

For contractions greater than 0.4%, Fig. 2 indicates a net densification for the processed fibers. As previously discussed, one problem with the Heat-Vacuum method was that as contraction increased, crystals began to appear on the fiber surface in greater number. The optical photographs of Fig. 3 show the growth morphology of these crystals with increasing temperature. Two distinct crystal types were observed: a large size with widths of ~50 μm and a small size with widths of ~2 μm. The irregular surfaces of the large size crystals plus the fact that crystals could be dislodged during handling were probably the major sources for the scatter in the high-contraction density data of Fig. 2. The fact both crystal types grew initially on the surface of the nodular of "kernel" structure of the as-received fiber can be seen by the scanning electron microscope (SEM) photographs of Fig. 4. Such growth supports the previously described low contraction model in that after the boron atoms diffused out of the sheath, they wandered along the surface until they nucleated to form crystals (7).

The structure of at least the large crystals was identified as the α-rhombohedral phase of boron from the fact that the diffraction lines for this phase were found in X-ray powder camera data on whole fibers such as that in Fig. 4. Because the density of α-boron is approximately 2.46 gm/cm^3 (9), it would appear then that the fiber densification observed at high contraction was produced by formation of dense surface crystals. Because the large crystals were observed to grow deep into the boron sheath by consuming adjacent material, it follows that growth of the surface crystals was also the probable source for the high contraction strains above 0.4%. The measured activation energy of 3.1 eV might then be associated with the energy required to convert the amorphous boron to the crystalline α-rhomboherdral boron.

To obtain an overall perspective of the above results and discussion, one can examine Fig. 5 which is a plot of fiber density versus one-hour heat treatment temperature. Upon initial heating above 800° C the as-

received density decreases slightly due to boron atom diffusion out of the sheath and onto the fiber surface where they form small crystals of α-rhombohedral boron. With further increases in temperature, the decreasing density reverses itself and increases due to the fact that as the surface crystals grow in number and size, they begin to consume adjacent material below the surface layers. This produces a rapid densification (and contraction) toward a ρ value equivalent to ~2.52 gm/cm^3 (α-boron plus core region). Near 1300^o C, the α crystals convert to β'-boron (8). Because X-ray diffraction data indicate that the amorphous lines remain up to 1500^o C, the 1320^o C fiber density is due to the β' and amorphous phases, microvoids and voids in the sheath, and the contribution from the tungsten boride core. Above 1500^o C, the β' and amorphous phases transform to β-rhombohedral boron, the phase stable at high temperature. The 1700^o C fiber density was slightly less than 2.41 gm/cm^3, the theoretical density calculated from the core contribution plus the β-boron density of 2.35 gm/cm^3 (10). This result might be explained by sheath microvoids and the fact that the fiber passed through many transformation steps, a process known to produce a β-boron phase slightly different than perfect β-boron (8). The approximate temperature regions for these transformation steps are indicated at the top of Fig. 5.

Heat-Argon Method

Table 2 lists contraction and density data for as-received 203 μm diameter boron fibers after heat treatment in argon gas. Four different treatment conditions were employed: pure argon/reactor, Ti-gettered argon/reactor, pure argon/furnace, and Ti-gettered argon/furnace. Each specimen was cleaned in methanol before heat treatment and before density measurement. Treatment-induced radial strains ϵ_r were measured from the initial and final effective diameters as determined from fiber mass, length, and density. For the reactor-heated fibers, initial diameters were determined from non-heated portions at either end of the reactor. In contrast to the Heat-Vacuum results, the final diameter data were not hindered by process-induced structure since the surfaces of

fibers heated in argon showed no visible change from the as-received nodular structure.

The first observation to be made from the Table 2 data is that purifying the argon gas significantly reduced the axial contraction. This result is clearly obvious in the furnace data where the same time-temperature conditions produced different ϵ_z. It is less obvious in the Ti-gettered argon/reactor data where for the particular conditions, contraction greater than 0.2% is expected by extrapolation of pure argon/reactor data at lower temperatures (1). The second observation is that the Heat-Argon method not only produced contraction in the axial and radial directions but also produced a decrease in fiber density. Thus fiber mass must have been lost either during the heat treatment or during the handling and cleaning procedures prior to the diameter and density measurements. A third observation is that at least for the two cases studied, the Heat-Argon method apparently produced uniform dilitation of the fiber, that is, $\epsilon_z = \epsilon_r$.

To explain the above observations, one might invoke a model in which during the Heat-Argon method boron atoms interacted with impurity gases in the argon, such as oxygen, to form a volatile phase at the processing temperatures and/or a solid phase which was completely removed during the subsequent cleaning in methanol. Loss of boron atoms from the large surface area of the fiber might then explain the diameter decrease but cannot account for the length decrease (unexposed fiber ends) or the fact of a density decrease. Thus the contractive ϵ_z can again be explained by atomic relaxation around microvoids which were generated by boron atom diffusion to the fiber surface. This model is supported by the fiber density data which show a monotonic decrease with increasing axial contraction. Finally the equality of ϵ_z and ϵ_r suggests that the microvoids produced uniform contraction. Thus most of the magnitude of ϵ_r was probably due not to surface layer removal but to microvoid production in the sheath.

The Table 2 data suggest that the driving force for microvoid production was the interaction between boron surface atoms and gaseous impurities in the argon. That is, purifying the argon reduced the boron-impurity interaction rate, thereby resulting in a drop in microvoid production as

manifested by a drop in axial contraction. This trend implies that if all impurities could be removed from the argon, no interaction should occur and no contraction should be observed. It seems, therefore, that impurity-free argon has a completely different effect on the fiber than impurity-free vacuum. A possible explanation might be that the presence of the gas inhibits either the boron atom surface diffusion or the crystal nucleation which occurs during vacuum heat treatment.

Basic Implications

Comparing the mechanistic models developed to explain contraction in vacuum and argon, one finds that in both cases contraction was produced by boron atom diffusion to the fiber surface. As the atoms emerged from the bulk of the boron sheath, the fiber contracted because the remaining microvoids had a smaller volume than the boron atoms as they existed in the sheath. In addition, it appears that the source of boron atoms and the manner in which they reached the fiber surface were the same for both methods. Striking evidence in support of such a conclusion can be found in the SEM photographs of Figs. 6(a) and (b) which show the growth of visible voids near the cores of fibers heat-treated in vacuum and argon, respectively. These results imply that boron atoms near the sheath-core interface somehow became involved in the surface processes which occurred during heat treatment. The exact physical mechanisms responsible for this behavior or the rapid diffusion by which boron atoms were able to participate in the surface phenomena have yet to be determined. Thus, at this time one can only speculate on these basic questions and offer possible models such as the following.

Within the amorphous fiber sheath, there exist two types of boron atoms: tightly-bound (TB) and loosely-bound (LB). The TB atoms are located in the regular structure of the 12-atom icosahedron, the structural subunit of all boron polymorphs. The LB atoms, which are not subject to the ordered constraints of the icosahedra, are located in regions of local disorder and thus are free to move rapidly through these regions. The high surface mobility of boron atoms (7) suggests that external and internal

surfaces within the sheath may be the disordered regions required for easy migration of the LB atoms. Thus, one might envision that at the start of the vacuum and argon heat treatments, LB atoms were migrating rapidly through all disordered regions of the fiber. Because proper conditions existed on the external fiber surface for nucleation and growth of α-boron crystals or for interaction with gaseous impurities, the local concentration of LB atoms decreased as they were absorbed into new phase formation. To maintain the equilibrium concentration, additional LB atoms moved rapidly onto the fiber surface, emerging from internal disordered regions such as kernel boundaries, interstices between icosahedra, and the interface between the sheath and core. This resulted in contraction due to microvoid formation within the sheath and near the core. Perhaps because there existed more disorder at the core interface, this region became the primary source of LB atoms. Thus, as contraction proceeded by the adsorption of LB atoms into surface phases, the number of microvoids increased with the highest concentration near the core interface. Eventually the microvoids coalesced to form the visible interfacial voids of Fig. 5 and possibly the dark regions along the kernel boundaries in Fig. 4(c).

Inherent in the above model is the concept that a two-step atomic process had to occur before the axial contractions could be observed. The first step is the thermally-activated removal of boron atoms from the fiber surface; the second step is the thermally-activated diffusion of boron atoms within the amorphous sheath. In our first report (1), the activation energies controlling Heat-Argon contractions were measured to be ~1.3 eV for contractions below 0.2% and ~0.8 eV for contractions greater than 0.3%. In light of the LB boron model, these results suggest that the diffusion energy for LB atoms is $\leq$1.30 eV in the as-received boron sheath and $\leq$0.8 eV in heat-treated sheaths which contain high concentrations of microvoids. These relatively low energies support the concept of rapid boron diffusion during heat treatment since they imply measurable diffusion beginning as low as 200^{o} C.

Besides developing a possible model to explain the qualitative features of the thermal treatment results, one can also use the similarity in contraction mechanisms to derive basic quantitative information concern-

ing microvoid production and microvoid properties in the heat treated fibers. Consider, for example, the changes in volume that occur when a number of boron atoms N' are removed from within the bulk of the boron sheath and placed on the fiber surface to form a surface phase X:

$$V_1 = V_0 + N'\Omega_X - \gamma N'\Omega_B \tag{1}$$

Here V_1 and V_0 are the final and initial fiber volumes, respectively; Ω_X is the atomic volume of the surface phase, Ω_B is the average atomic volume for the removed atoms as they existed in the sheath, and the parameter γ is a measure of the average change in fiber volume that occurs when bulk atoms relax around the microvoids formed by the removed atoms. Thus for no relaxation $\gamma = 0$, and for complete relaxation $\gamma = 1$. Defining $C' = N'/N_0$ as the concentration of removed atoms, one can rewrite Eq. (1) as

$$V_1/V_0 = 1 + C'[(\rho_B/\rho_X) - \gamma] \tag{2}$$

where the equalities $V_0 = N_0\Omega_B$ and $\Omega_X/\Omega_B = \rho_B/\rho_X$ were assumed.

For the Heat-Vacuum method, it appears that the above theory for volume change could apply during the early stages of contraction where small surface crystals are formed by atoms from within the bulk rather than from the material in adjacent surface layers Since no fiber mass was lost during vacuum processing, Eq. (2) predicts that at low ϵ_z, density should decrease according to

$$\rho_1/\rho_0 = 1 - C'[(\rho_B/\rho_\alpha) - \gamma] \tag{3}$$

where ρ_1, ρ_0, and ρ_α are, respectively, the final fiber density, initial fiber density, and the density of the α-rhombohedral surface crystals.

For the Heat-Argon method the interaction phase was removed so that $\Omega_X = 0$ and

$$M_1/M_0 = 1 - C' \tag{4}$$

where M_1 and M_0 are the final and initial fiber mass, respectively. Thus for this processing method, density should decrease at low ϵ_z according to

$$\rho_1/\rho_0 = 1 - C'(1 - \gamma) \tag{5}$$

If one neglects the small difference between ρ_α and ρ_B, Eqs. (3) and (5) indicate that at low contraction the density variation for the Heat-Vacuum and Heat-Argon methods should have the same dependence on C'. Assuming this to be the case and also a linear relation between the removed atom concentration and axial contraction, i.e.,

$$C' = -\lambda\epsilon_z \tag{6}$$

it follows that

$$\rho_1/\rho_0 = 1 + \epsilon_z[\lambda(1 - \gamma)] \tag{7}$$

where ϵ_z is negative. Plotting the low strain data of Tables 1 and 2 against ϵ_z, one obtains the results shown in Fig. 7. Best fitting these data to the linear dependence of Eq. (6), one finds that

$$\lambda(1 - \gamma) = 1.1 \pm 0.5 \tag{8}$$

But for the Heat-Argon method uniform contraction can be assumed so that

$$V_1/V_0 = 1 - C'\gamma = 1 + 3\epsilon_z \tag{9}$$

Thus,

$$\lambda = 3/\gamma = 4.1 \pm 0.5 \tag{10}$$

and

$$\gamma = 0.74 \pm 0.09 \tag{11}$$

The λ result indicates that during initial processing by the Heat-Vacuum and Heat-Argon methods, atoms were removed from the boron sheath at concentration levels of about a factor of four larger than the magnitude of the axial contraction strain. Thus, for example, those fibers whose strengths were increased from 4.3 to 5.5 GN/m^2 by axial contractions of 0.3%, the concentration of removal atoms was at least 1.2%.

The γ result indicates that there is a large relaxation of surrounding material into the microvoid left by a removed atom. The original volume of the removed boron atom Ω_B is reduced on the average by a factor of γ, resulting in a microvoid volume of only $0.26 \pm 0.09\ \Omega_B$. By comparison, the volume of a vacancy in a copper lattice is $\sim 0.4\ \Omega_{Cu}$ (11). Defining C_v as the volume fraction of microvoids in a contracted fiber, one finds that

$$C_v = (1 - \gamma)C' = (1.1 \pm 0.5)\epsilon_z \qquad (12)$$

This result implies, for example, a microvoid volume fraction of ~0.9% for the heat-treated fiber of Fig. 6(b). If all the microvoids were assumed to be contained in the visible voids around the core, an annular ring of voids of ~5 μm thickness should be expected. The average thickness estimated from Fig. 6(b) is ~2 μm, indicating that the majority of microvoids existed within the bulk of the boron sheath.

Recently Wawner (12) has observed a similar growth of visible voids at the sheath-core interface of 102 μm boron fibers heat-treated in various gaseous environments. Since these voids were accompanied by contractions up to 4%, it is believed that Heat-Argon mechanism of this study was also operating in Wawner results. Equation (12) suggests that microvoid volume fractions over 4% were produced in Wawner's fibers.

During the chemical vapor deposition of boron fibers, large axial elongations occur which are a drawback to increased fiber production (12). Mehalso (13) has suggested that the mechanism responsible for elongation is boron atom diffusion from deposited layers into the sheath which contains a high concentration of "vacancies." Atomic replacement of vacancies, which exist because of the rapid deposition conditions, produces a fiber volume increase and an axial elongation. In support of this elonga-

tion model, DiCarlo (5) has shown that the outer layers of the as-fabricated fiber have densities less than the average sheath density, suggesting a microvoid concentration gradient which decreases toward the core. The results presented here also support the Mehalso model in that they show that significant boron atom diffusion can occur within the sheath and that large volume changes are to be expected when a boron atom replaces a boron "vancancy." In fact, in many respects elongation might be considered the exact opposite of contraction as observed during argon processing.

Practical Implications

In light of the proceeding results and discussion, let us now attempt to understand how the sheath mechanisms operating during heat treatment affect boron fiber strengthening.

In our initial work (1) it was determined that the mechanical source of strength improvement was contraction of the total fiber and compression of the tungsten boride core. In this present work it was determined that the physical source of fiber axial contraction was boron atom removal from the sheath accompanied by the production of a microvoid with a much smaller atomic volume. The outward diffusion of boron atoms to the fiber surface produced a high concentration of microvoids near the core which eventually coalesced to form visible voids. Obviously, from a strength point of view, the growth of voids during secondary processing is an undesirable situation. When large enough, these voids can become flaws which induce fiber fracture at stresses lower then the fracture stresses associated with flaws within the compressed core. Thus, at some critical contraction strain, the advantages gained by compressing the core can no longer be realized.

Determination of the critical contraction strain ϵ_z^* by theoretical means is difficult. Studies on the relation between flaw size and boron fiber fracture stress suggest that a critical void diameter of $\sim 0.1\ \mu m$ is required to initiate sheath fracture below 6 GN/m^2 (14). Although in this work an equation relating ϵ_z and microvoid volume fraction C_v, was developed, relationships between C_v and the diameter of voids near

the core were not determined. For this reason it must be concluded that the practical limit of 0.3% observed for the fracture strain increase is a good empirical value for ϵ_z^*. This conclusion is supported by the observance that the low strength fracture sources for fibers contracted over 0.3% were actually located near the core (1). Additional evidence can be seen in Fig. 6(b) where at $\epsilon_z = -0.8\%$ the largest void diameter was measured to be ~3 μm, a value well in excess of the critical void diameter.

From the above discussion it follows that the practical limit of 0.3% is a natural consequence of the contraction or strengthening process. Thus, for at least 203 μm boron fibers, secondary heat treating techniques can produce fiber strengths only up to about 5.5 GN/m^2. This would apply also to other boron on tungsten fibers if their fracture is core-initiated and their microvoid level after fabrication is about the same as that of the 203 μm fiber. As discussed in our first report (1), the heat treatment in argon technique appeared to be the more cost-effective method because only slight surface etches were required after processing and because contraction rates were rapid. The etching was needed to eliminate surface flaws in the as-received fiber and surface flaws introduced by the interaction phase. The observation in this study that contraction was controlled by gaseous impurities suggests that even faster processing rates can be achieved by increasing the impurity level of the argon.

The basic method of improving boron fiber strength by heat-induced axial contraction appears to apply also to fiber surface environments other than vacuum and argon. For example, during secondary processing procedures to coat fibers with boron-nitride (15) and boron carbide (16), fracture stress histograms were uniformly shifted up to higher stresses by amounts which correspond to fracture strain increases of ~0.2%. The results presented here suggest that during the high temperature coating process, fiber contraction was probably occurring due to rapid boron atom diffusion through deposited layers of the coating phase. Also, during the heat treatment of boron/aluminum composities in the temperature range where boron and aluminum interact, increases in composite strength have been observed (17). Although improvements in interfacial bonding

may also have been occurring, it is possible that the boron fibers were contracting due to boron atom diffusion out of the fibers and into the aluminum matrix. In support of this, recently obtained internal friction data (18) suggest that during B/Al fabrication boron atoms do enter into the bulk of the matrix. Data indicating that the outward diffusion of boron atoms occurs in boron/titanium composities have also been obtained (19). Thus it is believed that due to the high mobility of boron atoms, boron fiber strengthening can be achieved in many high temperature environments as long as an interaction mechanism exists for removal of boron atoms from the surface. Obviously this strengthening can be realized only if the interaction mechanism does not introduce any new low-strength surface flaws.

SUMMARY

The mechanical and physical mechanisms responsible for improving the strength of commercial 203 μm boron on tungsten fibers by heat treatment have been identified. Because fracture of these fibers is core-initiated, the mechanical mechanism is thermally-induced axial contraction of the entire fiber and compression of the core region. Fiber fracture strain is thus increased by an amount equal to the axial contraction. The physical mechanism operating during fiber contraction is boron atom diffusion out of the boron sheath. Replacement of a boron atom with a boron microvoid results in a volume decrease as manifested by equal axial and radial contractions.

In high vacuum processing, the driving force for boron atom removal appears to be the formation of surface crystals. In argon gas processing, the driving force is probably the interaction between boron atoms and gaseous impurities in the argon. As the atoms leave the sheath they produce microvoids with the highest concentration near the core. Eventually the microvoids nearest the core coalesce to form visible voids which, because of their flaw type nature, limit fraction strain increases to 0.3%. Thus by heat treating in impure argon, which appears to be cost effective, boron fiber strengths can be increased up to 5.5 GN/m^2 with a coefficient of variability of less than 5%.

REFERENCES

1. J. A. DiCarlo, "Techniques for Increasing Boron Fiber Fracture Strain," NASA TM X-73627, 1977.

2. R. J. Smith, "Changes in Boron Fiber Strength Due to Surface Removal by Chemical Etching," NASA TN D-8219, 1976.

3. D. R. Behrendt; pp. 215-226 in Composite Materials; Testing and Design. ASTM-STP-617, American Society for Testing Materials, Philadelphia, 1977.

4. V. Krukonis, pp. 517-540 in Boron and Refractory Borides. Edited by V. I. Matkovich, Springer-Verlag, Berlin, 1977.

5. J. A. DiCarlo, pp. 520-538 in Second International Conference on Composite Materials. American Institute of Mechanical Engineers, New York, 1978.

6. Thermophysical Properties of High Temperature Solid Materials, Vol. 1. Edited by Y. S. Touloukian, MacMillan Company, New York, 1967.

7. J. S. Gillespie, Jr., "Crystallization of Massive Amorphous Boron," J. Am. Chem. Soc., 88, 2423-2425 (1966).

8. P. Runow, "Study of the α to β Transformation in Boron," J. Mater. Sci., 7, 499-511 (1972).

9. L. V. McCarty, J. S. Kasper, F. H. Horn, B. F. Decker, and A. E. Newkirk, "A New Crystalline Modification of Boron," J. Am. Chem. Soc., 80(10), 2592 (1958).

10. D. E. Sands and J. L. Hoard, "Rhombohedral Elemental Boron," J. Am. Chem. Soc., 79(20), 5582-5583 (1957).

11. A. C. Damask and G. J. Dienes, Point Defects in Metals. Gordon and Breach, New York, 1963.

12. F. E. Wawner, Jr., "Investigation of Elongation and Its Relationship to Residual Stresses in Boron Filaments," Univ. of Virginia Report No. UVA/525322/MS78/101, 1978.

13. R. Mehalso, "Chemical Vapor Deposition of Boron on a Carbon Monofiliment Substrate - A Study of Residual Stresses and Deposition Kinetics," Ph. D. Dissertation, Rensselaer Polytechnic Inst., Troy, N. Y., 1974.

14. J. Vega-Boggio, J. Schweitz, and O. Vingsbo, "Surface Energy Measurements from Griffith Cracks in Boron Fibers," J. Mater. Sci., 12, 1692-1693 (1977).

15. J. L. Camahort, V. J. Krukonis, and F. E. Wawner, "Low Cost B-Al Composites by Cast Tape," SAMPE Q, 6, 40-43 (1975).

16. Boron Carbide (B_4C) Coated Boron Filaments, for Metal Matrix Applications. AVCO Specialty Materials Division, Lowell, Mass.

17. A. G. Metcalfe and M. J. Klein, pp. 125-168 in Composite Materials, Vol. 1. Edited by A. G. Metcalfe, Academic Press, New York, 1974.

18. J. A. DiCarlo and J. E. Maisel, "High Temperature Dynamic Modulus and Damping of Aluminum and Titanium Matrix Composites," NASA TM-79080, 1979.

19. J. Thebault, R. Pailler, G. Bontemps-Moley, M. Bourdeau, and R. Naslain, "Chemical Compatability in Boron Fiber-Titanium Composite Materials," J. Less-Common Metals, 47, 221-233 (1976).

TABLE 1 - HEAT-VACUUM METHOD: CONTRACTION AND DENSITY RESULTS[a]

Treatment conditions		Average axial strain	Average density
Temperature, °C	Time, min	ϵ_z, %	ρ, gm/cm^3
As-received		[b] 0	[c] 2.4099±0.0003 (3)
1000	6	[c] -0.144±0.012 (3)	
1095	6	-0.255±0.020 (2)	2.4085±0.0003 (1)
1205	6	-0.599±0.043 (4)	2.4165±0.0003 (1)
915	60	-0.106±0.022 (4)	
995	60	-0.280±0.018 (4)	
1090	60	-0.670±0.005 (2)	2.4237±0.0024 (2)
1185	60	-1.063±0.069 (4)	2.5076±0.0010 (1)
900	600	-0.222±0.014 (4)	2.4083±0.0003 (1)
995	600	-0.751±0.014 (2)	2.4374±0.0019 (2)
1320	60		2.3907±0.0031 (3)
1700	60		2.4041±0.0015 (2)

[a]Specimens were as-received 203 μm boron on tungsten fibers.
[b]Axial strain of the as-received fiber was taken as zero.
[c]Number in parenthesis indicates number of specimens employed for the measurement.

TABLE 2. - HEAT-ARGON METHOD: CONTRACTION AND DENSITY RESULTS[a]

Treatment conditions			Axial strain ϵ_z, %	Radial strain ϵ_r, %	Average density ρ, gm/cm^3
	Temperature, °C	Time, min			
As-received			[b]0	[b]0	[c]2.4099±0.0003 (3)
Reactor					
Pure argon	947	130	-0.67	-0.66±0.03	2.4063±0.0003 (1)
	900	240	-0.82	-0.78±0.04	2.4003±0.0021 (4)
Ti-gettered argon	1180	2	-0.11		2.4072±0.0003 (1)
Furnace					
Pure argon	1190	6	[c]-0.44(3)		
Ti-gettered argon	1190	6	-0.11(3)		

[a]Specimens were as-received 203 μm boron on tungsten fibers.

[b]Axial and radial strains of the as-received fiber were taken as zero.

[c]Number in parenthesis indicates number of specimens employed for the measurement.

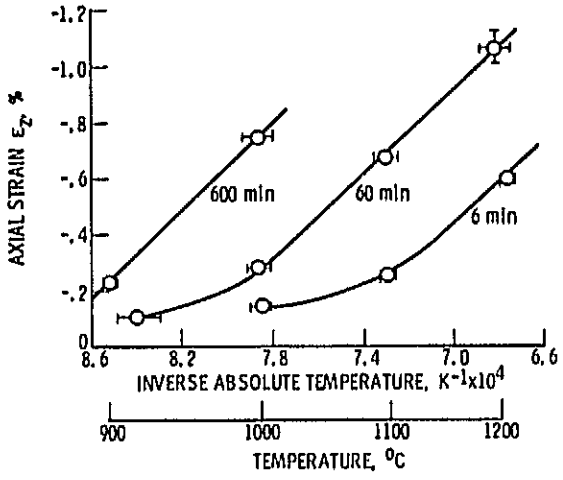

Figure 1. - Axial contraction produced in 203 μm boron on tungsten fibers by heat treatment under high vacuum.

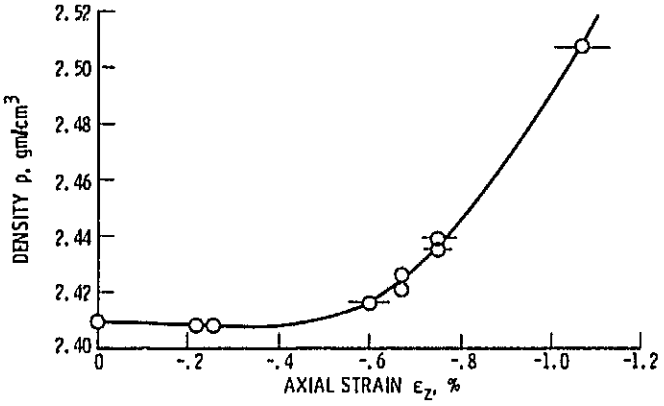

Figure 2. - Dependence of fiber density on the axial contraction produced in 203 μm boron on tungsten fibers by heat treatment under high vacuum.

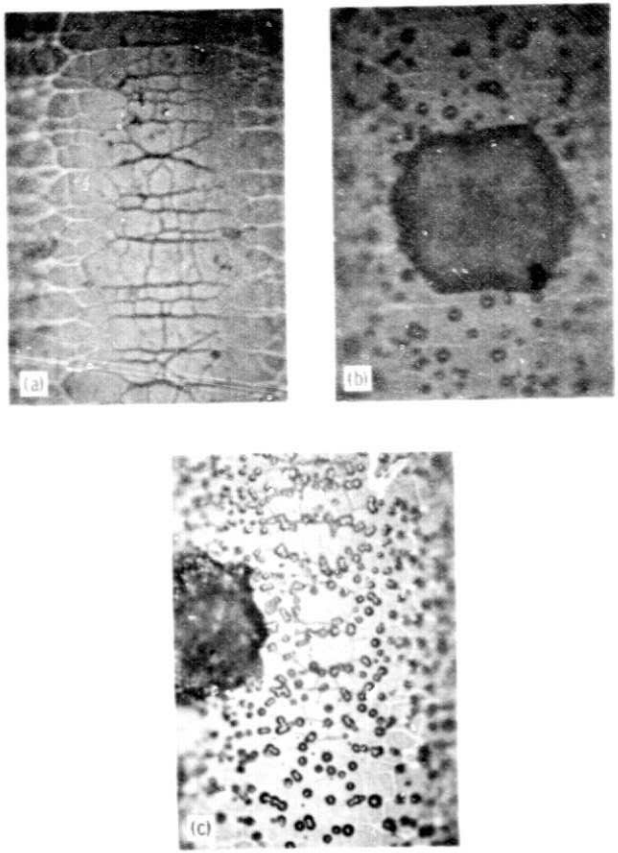

Figure 3. - Optical microscope photographs of boron fiber surfaces in the as-received condition (a) and after high vacuum heat treatment for one hour at (b) 1040^0 C and (c) 1340^0 C. Magnification factors are 1000.

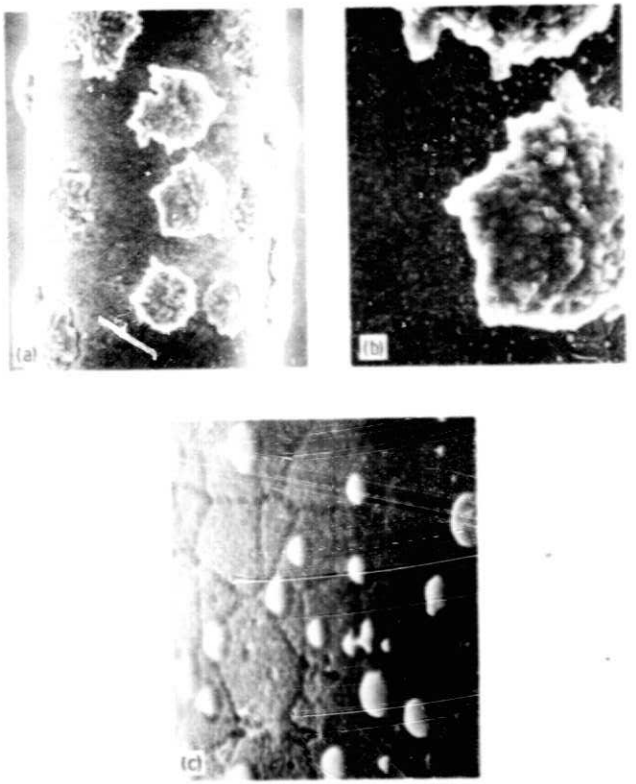

Figure 4. - Scanning electron microscope photographs of surface crystal growth on a boron fiber heat treated under vacuum for one hour at 1170^0 C. Approximate magnification factors are (a) 300, (b) 1000, and (c) 3000.

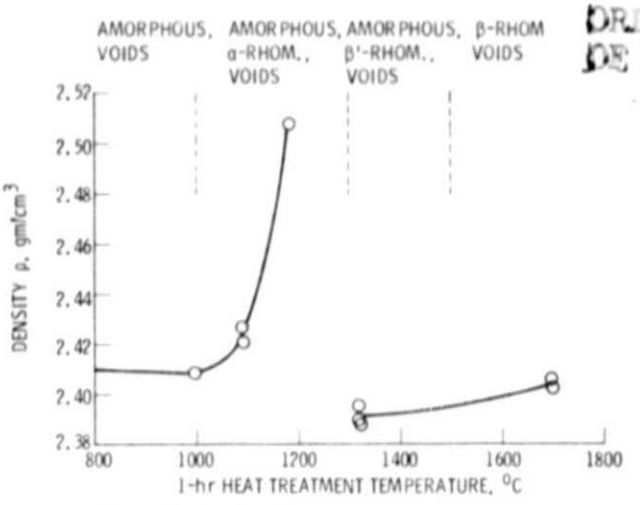

Figure 5. - Density of 203 μm boron on tungsten fibers after 1-hr heat treatment under high vacuum. Also indicated are the approximate stability ranges for the boron structure assumed to be responsible for the density variation.

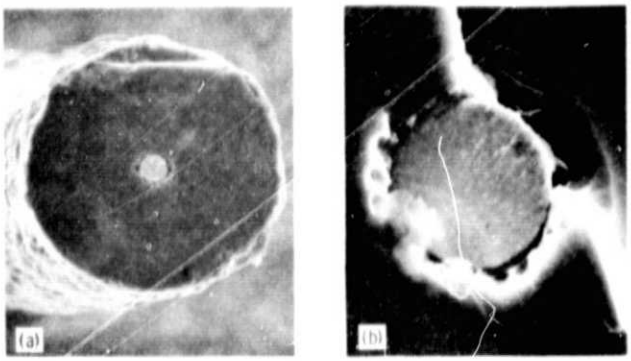

Figure 6. - Scanning electron microscope photographs of sheath voids near the cores of 203 μm boron on tungsten fibers after heat treatment (a) under high vacuum at 1320° C and (b) under argon at 900° C (axial contraction of 0.8%). Approximate magnification factors are (a) 300 and (b) 3000.

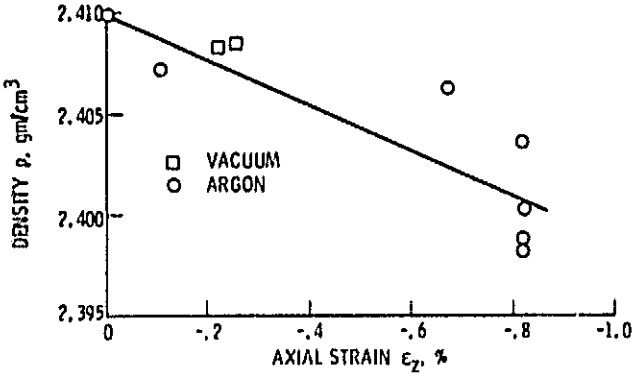

Figure 7. - Dependence of fiber density on the axial contraction produced in 203 μm boron on tungsten fibers by heat treatment under argon and high vacuum.